

Supergiant porphyry copper deposits are failed large eruptions

Massimo Chiaradia ¹✉ & Luca Caricchi ¹

Porphyry copper deposits, the principal source of copper and molybdenum, form at convergent margins. Copper is precipitated from fluids associated with cooling magmas that have formed in the mantle and evolved at mid- to lower crustal levels, before rising toward the surface where they saturate and exsolve an aqueous fluid and copper. Despite advances in the understanding of their formation, there are still underexplored aspects of the genesis of porphyry copper deposits. Here we examine the role played by magma injection rates into the upper crust on the formation of porphyry copper deposits with different copper endowments. Mass balance calculations suggest that supergiant porphyry copper deposits (>10 million tonnes copper) require magma volumes (up to >2500 km³) and magma injection rates (>0.001 km³ year⁻¹) typical of large volcanic eruptions from rift, hot spot, and subduction-related settings. Because large volcanic eruptions would destroy magmatic-hydrothermal systems or prevent their formation, the largest porphyry copper deposits can be considered as failed large eruptions and this may be one of the causes of their rarity.

¹Department of Earth Sciences, University of Geneva, Rue des Maraîchers 13, 1205 Geneva, Switzerland. ✉email: Massimo.Chiaradia@unige.ch

The last decades have seen a continuous increase in the understanding of how porphyry copper deposits form. Several studies have unveiled the different processes that control the formation of porphyry copper deposits, including geodynamic setting, tectonics, magma genesis, magma evolution, and fluid chemistry^{1–14}. Recent work¹³ has shown that Cu-rich porphyry copper deposits occur in association with syn-subduction calc-alkaline magmas in thick continental arcs. In contrast, Au-rich porphyry copper deposits preferentially occur in association with variably alkaline rocks in complex settings, such as post-subduction in continental and thinner island arcs. In this study we focus exclusively on the syn-subduction Cu-rich porphyry copper deposit type (hereafter referred to as porphyry copper deposits), occurring in thick continental arcs.

Recent efforts have been directed towards a physical understanding of the processes leading to the formation of porphyry copper deposits through thermodynamic and petrologic modelling^{15–18}. Simple mass balance constraints are useful to set quantitative boundaries within which various processes interact to form porphyry copper deposits. Arc magmas are characterized by a narrow range of Cu contents^{19,20} and fluid-melt partition coefficients for Cu are also limited to a relatively restricted range²¹. Thus, purely from mass balance considerations, the main parameter determining the size of a porphyry copper deposit (considering similar precipitation efficiencies from the hydrothermal fluid²²) is the mass of fluid, which, in turn, is closely associated with the mass of degassing magma^{16,17}. The model¹⁷ uses the Cu concentrations of magmas in thick (>30 km) arcs as constrained by several thousands of analyses on recent arcs²⁰. Magmas in thick arcs undergo a continuous depletion during crustal differentiation, and intermediate to felsic magmas, typically associated with porphyry copper deposits, contain 20–50 ppm Cu¹⁷. Therefore, in order to form supergiant porphyry copper deposits the relatively low Cu contents of thick arc magmas need to be compensated by large volumes of magma accumulated in the mid- to lower crust¹⁷ (depths >15 km; Fig. 1). The resulting model¹⁷ is consistent with trace element geochemistry (e.g., Sr/Y), timescales of magmatic processes associated with porphyry copper deposits (long precursor magmatic activity in the mid- to lower crust), and volumes of magma associated with mineralization inferred from fluid inclusion chemistry and geophysical constraints²³. Other models advocate the need of Cu-rich magmas²⁴, but the lack of a systematic record of Cu enrichment in thick arc magmas²⁰, while not excluding it, make this process less likely. Recycling of Cu-sulphides⁹ is also possible, but sulfide pre-concentrations would require extraction of Cu from large amounts of low-Cu thick arc magma, falling back in the model of¹⁷.

However, the accumulation of large magma volumes at mid- to lower crust depths (Fig. 1) does not guarantee the formation of a porphyry copper deposit. This is confirmed by the absence of a relationship between the duration of magma accumulation at mid- to lower crustal levels^{25–28} and the Cu endowments of porphyry copper deposits (Fig. 2).

Magmas in the mid- to lower crust are mostly H₂O-undersaturated, because of the strong pressure dependency of H₂O solubility in silicate melts²⁹. The exsolution of mineralising fluids requires magma ascent to upper crustal levels, in the so-called parental magma reservoir^{22,30} (~5–15 km depth; Fig. 1), which feeds the porphyry apophyses around which mineralization commonly occurs at depths < ~6 km (Fig. 1).

Despite more high-precision and accurate geochronological data are needed, a broad correlation^{13,16,17,31} suggests that a longer period of the overall ore-forming process will result in a larger Cu endowment of the deposit (Fig. 3). In particular, it is recognized that the largest porphyry copper deposits (>~40 Mt Cu) are formed

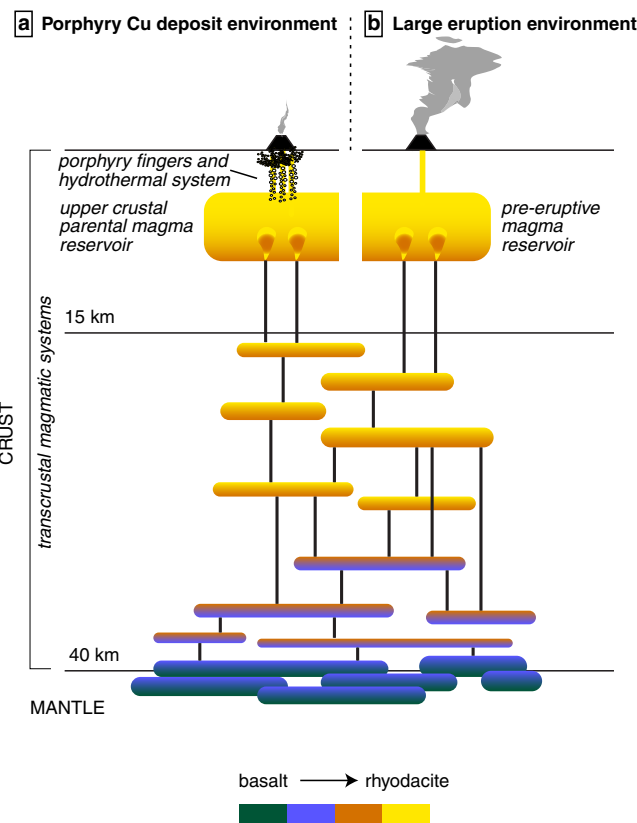


Fig. 1 Transcrustal magmatic systems associated with porphyry copper deposits and with large eruptions. **a** Transcrustal magmatic systems associated with porphyry copper deposits. **b** Transcrustal magmatic systems associated with large eruptions. The sketch highlights the similarities between the two systems and is inspired from sketches of previous works^{17,33,35,64,69}. The ~40 km depth is indicative and used for consistency with the model which is run for a maximum pressure of 1.2 GPa.

by superposition of repeated magmatic-hydrothermal events over time spans of up to >1 Myr¹³ (Fig. 3). Therefore, ultimately the endowments of porphyry copper deposits depend on the efficiency of transfer of the largest possible magma volumes from the mid- to lower crust into the shallow parental magma reservoir feeding the porphyry apophyses around which ore deposition occurs (Fig. 1).

Here, we show that Cu endowments of porphyry copper deposits increase with volumes and rates of magma transfer from the mid- to lower-crust into the shallow parental magma reservoir. The largest porphyry copper deposits require magma volumes (from several hundreds to a few thousands km³) and injection rates into the upper crustal parental magma reservoir (>0.001 km³ yr⁻¹) that are similar to those leading to large eruptions in rift-, hot-spot, and subduction-related settings^{15,32–35} (Fig. 1). Because volcanic eruptions are detrimental for magmatic-hydrothermal systems, as they would either destroy them or prevent their formation^{36–38}, the largest porphyry copper deposits can be considered failed large eruptions.

Results and discussion

Model rationale and constraints. We used two simple constraints to obtain average magma injection rates from the mid- to lower crust accumulation zone into the upper crustal magma reservoir above which mineralization takes place (Fig. 1): (i) the volume of magma required to precipitate a specific Cu mass, with a conservative precipitation efficiency of 50%²²; (ii) the time

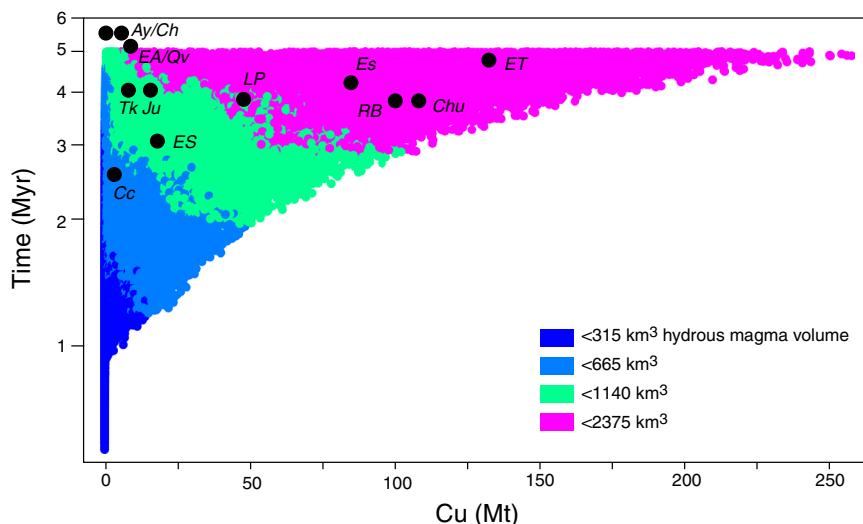


Fig. 2 Cu endowments (Mt) versus duration of magma injection into the crust. Plot showing Cu endowments (Mt) versus duration of magma injection into the crust (Myr). Colored dots are 50% precipitation efficiency simulations from¹⁷ and different colors indicate the volumes of the magma accumulated as specified in the legend. The black dots are porphyry copper deposits for which data are available for Cu endowments and duration of magmatic activity^{13,17} (Supplementary Data 1). Ay Antapaccay, Ch Chaucha, Chu Chuquicamata, Cc Corocochuayco, Es Escondida, EA El Abra, ES El Salvador, ET El Teniente, Ju Junin, LP Los Pelambres, Qv Quellaveco, RB Rio Blanco, Tk Tampakan.

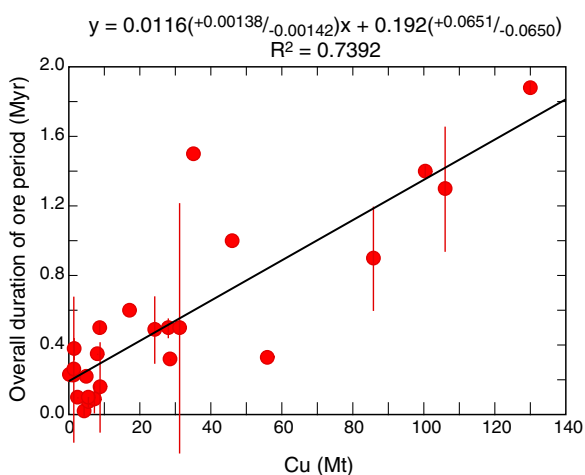


Fig. 3 Relationship between the overall duration of ore period and Cu endowments. Plot showing the relationship between the overall duration of the ore period (Myr) and Cu endowments (Mt) of porphyry copper deposits. The data from porphyry copper deposits (Cu Mt, ore durations and associated 1SD uncertainty bars) are from Supplementary Data 1. Overall durations of the ore periods are the calculated differences between the oldest and youngest ages of recorded magmatic-hydrothermal mineralizing events with their propagated uncertainties where uncertainties on the above ages are available. The equation reported is the best-fit linear regression between the two variables with associated uncertainties for the slope and intercept.

interval within which such magma volume is transferred from the mid- to lower crust accumulation zone (i.e., >~15 km depth) into the upper crust (i.e., 5–15 km depth) where Cu is precipitated. The ratio between these two parameters gives the average magma injection rate corresponding to a specific Cu endowment.

Magma volume and Cu endowments. Point (i) above is constrained by the relationship between potential Cu endowments of transcrustal magmatic systems and the volume (mass) of magma accumulated in the mid- to lower crust^{13,17} (Methods and

Table 1). Modelling¹⁷ indicates that the largest potential Cu endowments are associated with magma accumulations occurring at pressures greater than 0.4 GPa (>~14 km depth) and for injection periods longer than 2.5–3.0 Myr.

The magmas accumulated at pressures greater than 0.4 GPa and up to 1.2 GPa (the maximum pressure modelled: Table 1) are characterized by relatively high H₂O contents (mostly in the range 6–12 wt.%), yet they are mostly H₂O-undersaturated at depths >0.4 GPa because of the strong pressure dependence of H₂O solubility in silicate melts²⁹. These magmas can release fluids and potentially lead to the formation of porphyry copper deposits only if they ascend to depths at which they become H₂O-saturated, i.e., between ~8 and 17 km¹⁷, which overlaps with the depth (5–15 km) of the parental magma reservoir^{22,30}. Fluid saturation would be achieved at greater depths if magma also contained CO₂²⁹; however, early exsolved fluids would be CO₂-rich³⁹ and represent a small contribution to the total mass of fluid released²⁹. For these reasons, in our calculations we simplistically consider that magmas contain exclusively H₂O and that the volumes of magma generated in the mid- to lower crust (0.4–1.2 GPa), which determine the maximum potential Cu endowment of the porphyry deposits¹⁷, are transferred up to their H₂O saturation depth interval, corresponding to the parental magma reservoir (Fig. 1). There, we consider that magmas release the entire amount of H₂O (and associated Cu through the random range, 2–100, of K_D values used in the model: Table 1), i.e., we consider that all H₂O is exsolved because of decompression and isobaric crystallization. This results in a slight overestimation of the exsolved H₂O since intermediate-felsic plutonic rocks may retain some H₂O in the form of hydrated minerals like amphibole and biotite. Such overestimation is largely compensated by the conservative 50% precipitation efficiency of Cu used in the model.

Figure 4 shows the expected broad positive correlation between potential Cu endowments and calculated magma volumes accumulated at mid- to lower crustal levels (i.e., at pressures between 0.4 and 1.2 GPa). The range of variable Cu endowments associated with a specific magma volume depends on: (1) the different depths at which magmas can accumulate in the model (0.4–1.2 GPa), which in turn controls the fluid content of the

Table 1 Constraints on the parameters used in the Monte Carlo modelling of magma injection rates.

Parameter	Range of values or value
Magma injection rate in the mid- to lower crust through a circular surface of 15 km diameter	0.0009 km ³ /yr ^a
Duration of magma injection in the mid- to lower crust	0–5 Myr ^b
Pressure at which magma injection occurs in the mid- to lower crust	0.4–1.2 GPa ^c
Potential Cu endowments in mid- to lower crust accumulated magma systems (MtCu)	0–150 Mt Cu ^d
K _D fluid-melt for Cu (K _D)	2–100 ^e
Mid- to lower crust magma volumes corresponding to a specific Cu endowment (within the random range above 0–150 Mt Cu) (MLC_magmaVol)	MLC_magmaVol = $a * \text{MtCu}^b$ (equation 1)
Parameter “a” in equation 1 above	60–700 ^f
Parameter “b” in equation 1 above	$b = -0.187767 * \ln(a) + 1.507068$ (equation 2)
Number of magma pulses transferring a mid- to lower crust magma accumulation corresponding to a specific Cu endowment to its H ₂ O saturation depth in the shallower crust (N_pulses) (see main text)	5–20
Duration of magma pulses transferring a mid- to lower crust magma accumulation corresponding to a specific Cu endowment to its H ₂ O saturation depth in the shallower crust (Pulse_duration) (see main text)	2000–100000 years
Magma volume of each pulse transferring a mid- to lower crust magma accumulation corresponding to a specific Cu endowment to its H ₂ O saturation depth in the shallower crust (Pulse_volume)	MLC_magmaVol/N_pulses (equation 3)
Duration of magma transfer from the mid- to lower crust to the shallow crust	Pulse_duration * N_pulses (equation 4)
Magma injection rate from the mid- to lower crust accumulation reservoir into the shallow crust	Pulse_volume/Pulse_duration (equation 5)

^aTypical average arc magma injection rate^{57,64}. See also¹⁷.

^{b, c} See¹⁷.

^d Data from <https://mrddata.usgs.gov/porcu/>. See also¹³ for a summary.

^e From⁶⁸.

^f This range corresponds to enveloping curves enclosing 95% of the data in the correlation between magma volumes accumulated in the mid- to lower crust and their potential Cu endowments exsolvable with fluids at H₂O saturation depth with a 50% precipitation efficiency for Cu (Fig. 4).

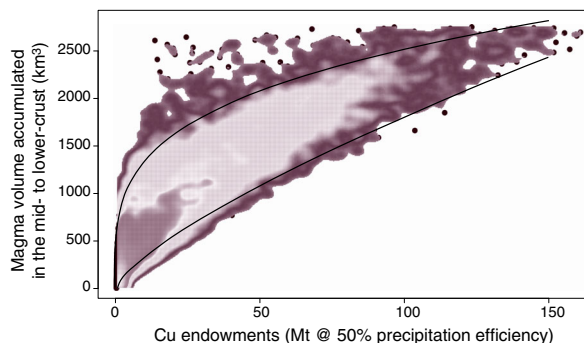


Fig. 4 Plot of magma volumes versus potential Cu endowments. Plot of magma volumes versus potential Cu endowments at 50% precipitation efficiency for magmatic systems accumulated at depths corresponding to pressures of 0.4–1.2 GPa. Over 10000 simulations are reported from the algorithm of^{13,17}. Density distribution is shown on top of the data as different color shades. More than 95% of the simulations fall within the two exponential curves, as discussed in the Methods and Table 1.

residual melt; (2) the different durations of magma injections (0–5 Myr), and, to a lesser extent, the range of K_D fluid-melt values for Cu used in the model (2–100). Since more than 95% of the simulations fall within the two exponential curves of Fig. 4, we have modelled the magma injection rates for the transfer of the magma volumes to the shallow crust comprised within these two curves (Table 1 and Methods). Figure 4 shows that the largest potential Cu endowments (>~20 and up to a maximum of 150 Mt Cu in the model, for a 50% precipitation efficiency) are associated with volumes of magma accumulated in the mid- to lower crust of >500 and up to ~2500 km³. These magma volumes are of the same order of magnitude as those explosively ejected by supereruptions³⁵.

Duration of ore deposition events. The second constraint of the model (ii) is provided by available geochronological data on the overall duration of ore deposition. Geochronological data indicate

that the overall ore deposition durations in the largest porphyry deposits are <~2 Myr (e.g., Chuquicamata 106 Mt Cu, 1.3 ± 0.36 Myr^{40,41}; El Teniente, 130 Mt Cu, 1.88 ± 0.04 Myr^{42,43}; Rio Blanco, 100.4 Mt Cu, 1.4 ± 0.04 Myr⁴⁴; Fig. 3). This translates into average Cu deposition rates at these deposits of 74 ± 7 Cu tonnes yr⁻¹. Taking into account all major porphyry copper deposits with available geochronological estimation of ore deposition duration¹³, the average rate of Cu deposition for all these deposits is 65 ± 7 Cu tonnes yr⁻¹ (Fig. 3). We reasonably assume that the overall duration of the mineralizing events constrains the duration of the magma injection from the mid- to lower crust into the upper crust (Methods). In order to comply with the above figures, in our model we have taken as a maximum temporal limit a duration of 2.0 Myr for the transfer into the upper crust of the magma volumes associated with deposition of up to 150 Mt Cu at 50% efficiency.

Magma injection rates. Models based on geological cross-cutting relationships^{45,46}, geochronology^{47–50}, geospeedometry based on element diffusion³¹, and thermodynamic⁵¹ as well as numerical modelling⁵² suggest that porphyry copper deposits are formed by multi-step magmatic-hydrothermal pulses, reflecting a variable number of magmatic intrusions and fluid release cycles. High-precision dating of both hydrothermal (e.g., molybdenite Re-Os dating) and magmatic activity (U-Pb dating of zircons) suggests that the duration of each pulse may be as short as a few tens of thousands or even a few thousands of years^{47–50,53}. These results are corroborated also by Ti diffusion in hydrothermal quartz, which indicates timescales of single pulses of magmatic-hydrothermal activity as short as a few thousands of years or even less³¹. Recent studies on Ti-in-quartz diffusivity^{54,55} suggest slower Ti diffusion rates in quartz (up to two orders of magnitude less than those taken into account by³¹). These would result in longer durations of single hydrothermal pulses, which, nonetheless, remain on the order of tens to hundreds of thousand years. Thermodynamic and numerical modelling agrees with timescales determined for individual magmatic-hydrothermal pulses as well^{51,52}.

We allow a random range of 5–20 pulses to inject, from the mid- to lower-crust into the upper crust parental reservoir, the magma volume required for the deposition of a specific amount of Cu (Fig. 4). We vary randomly the duration of the single magma pulse transfer events between 2000 and 100000 years to comply with the available geochronological data discussed above.

The transfer of the magma volume corresponding to a specific Cu endowment from the mid- to lower crust to the parental magma reservoir is accomplished through random combinations of fixed magma volume pulses and fixed durations of the magma pulse within the combination of 2000–100000 years pulse duration and 5–20 number of pulses, corresponding to a maximum possible duration of 2.0 Myr and a minimum of 10000 years. It follows that each simulation represents an average magma injection rate that results in the transfer of a specific magma volume and associated Cu endowment from the deep accumulation zone to the shallow crustal reservoir (Fig. 1). Five hundred thousand simulations were performed (Table 1) using the RStudio script⁵⁶ provided in the Supplementary Note 1.

Magma injection rates in supergiant porphyry copper deposits.

The average rate of magma injection into the upper crust controls whether magma will rapidly cool and form plutonic intrusions or whether it will accumulate and form variably large reservoirs that eventually may erupt catastrophically^{15,32,57,58}. Recent studies have started to include magma injection rates in the formation models of porphyry deposits^{15,16,38}. Intuitively, high magma injection rates favor explosive volcanic eruptions^{15,32,57,58} and are detrimental for the formation of porphyry deposits^{36–38}. This is supported by the occurrence of porphyry-type deposits at the end of variably long periods of precursor volcanic activity and coinciding with periods characterized by the lack of or by very low volcanic activity (e.g., Yanacocha⁵⁹). In contrast, magma injection rates that allow the accumulation of magma at shallow levels without its eruption may eventually result in a magmatic system exsolving fluids and generating a mineralized magmatic-hydrothermal system³⁸. However, there are no studies that have addressed, quantitatively and on a global scale, how and if different rates of magma injection, encompassing the broad range below the threshold of those leading to eruption, control the formation and size of porphyry deposits.

Figure 5 shows simulations of magma volume versus magma injection rate. Also shown are the fields corresponding to large porphyry copper deposits based on zircon age distribution modelling¹⁵, those corresponding to various individual porphyry copper deposits based on combination of hydrothermal and magmatic activity durations¹⁶, and the field for the Bingham Canyon porphyry deposit, as inferred from geochemical and thermal modelling of zircons⁶⁰. Our constrained magma injection rates overlap with the variably broad ranges defined by these previous studies (~ 0.0001 – $0.04 \text{ km}^3 \text{ yr}^{-1}$), but further constrain the magma injection rates associated with specific porphyry copper deposits, excluding lower magma injection rates (Fig. 5). Figure 5 further shows that larger Cu endowments require larger minimum magma injection rates to transfer increasingly larger amounts of magmas and Cu from the mid- to lower crust accumulation zone to the shallow parental reservoir within the timescales constrained by geochronology. All simulations for the largest possible Cu endowments ($>100 \text{ Mt Cu}$) require magma injection rates higher than $\sim 0.001 \text{ km}^3 \text{ yr}^{-1}$ (Fig. 5). Additionally, the broadly normal density distributions of the simulations for various Cu endowment intervals (<10 , 10–30, 30–50, 50–70, 70–100, $>100 \text{ Mt}$; Supplementary Fig. 1) show that all the Cu endowment intervals $>10 \text{ Mt Cu}$ (supergiant porphyry copper deposits according to the nomenclature of⁶¹) require mode values

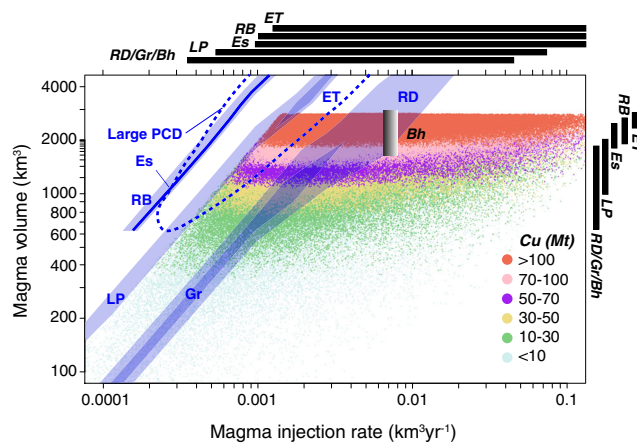


Fig. 5 Monte Carlo simulations of magma volumes versus injection rates.

Monte Carlo simulations of magma volumes versus injection rates subdivided by color codes indicating different intervals of potential Cu endowments. The blue fields and associated blue labels correspond to individual porphyry copper deposits from combination of hydrothermal and magmatic activity ages of the deposits¹⁶, the field enclosed by the blue dashed line is the field of large porphyry copper deposits (PCD) based on zircon age distribution modelling¹⁵, and the Bingham Canyon (Bh) value is inferred from geochemical and thermal modelling of zircons⁶⁰. The black bars (and associated black labels) correspond to the magma volumes and magma injection rate intervals constrained by the present study on the basis of Monte Carlo simulations for the same individual deposits of^{16,60}. Es Escondida, ET El Teniente, Gr Grasberg, LP Los Pelambres, RB Rio Blanco, RD Reko Diq.

of magma injection rates, i.e., the statistically most recurrent value in our simulations, higher than $0.001 \text{ km}^3 \text{ yr}^{-1}$. For instance, the mode value of magma injection rates for porphyry copper deposits with $>100 \text{ Mt Cu}$ is $>0.003 \text{ km}^3 \text{ yr}^{-1}$ (Supplementary Fig. 1).

The rates of magma transfer to the upper crust obtained here are minimum values, because the overall ore deposit durations considered are maximum values, bracketing the beginning and end of the mineralizing process. If, within these temporal intervals, most of the copper is precipitated within shorter timescales, the magma injection rates would be higher than those obtained here. Conversely, the rates of magma transfer would decrease, at equal overall duration of the mineralization, for deposits with a higher Cu precipitation efficiency than the one used here (50%)²². Nonetheless, the broadly linear correlation between Cu endowments and duration of ore deposition for porphyry copper deposits (Fig. 3) suggests that precipitation efficiencies are probably similar for most porphyry copper deposits.

Also in the ore duration versus Cu endowment space (Fig. 6) our results show that all porphyry copper deposits require magma injection rates >0.0010 and up to at least $\sim 0.0022 \text{ km}^3 \text{ yr}^{-1}$ (i.e., $10^{-3.0}$ and $10^{-2.65} \text{ km}^3 \text{ yr}^{-1}$, respectively, in Fig. 6). This is in agreement with recent work³⁸, suggesting that magma injection rates higher than $0.0013 \text{ km}^3 \text{ yr}^{-1}$ are necessary to form porphyry copper deposits. The minimum upper limit of the magma injection rate interval (~ 0.0022 , i.e., $10^{-2.65} \text{ km}^3 \text{ yr}^{-1}$), appropriate for the formation of most porphyry copper deposits according to our simulations, falls in the range of magma injection rates into the upper crust that lead to large eruptions^{15,32–34}. The lower limit ($\sim 0.001 \text{ km}^3 \text{ yr}^{-1}$) corresponds to the highest possible magma injection rates that may result in the build-up of non-eruptible (i.e., plutonic) magma bodies at upper crustal levels¹⁵. However, an important aspect to consider

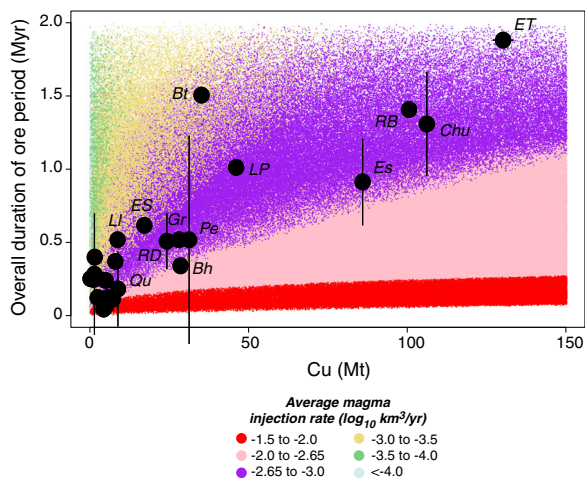


Fig. 6 Monte Carlo simulations of duration of ore deposition versus Cu endowments. Monte Carlo simulations of duration of ore deposition (which also correspond to duration of magma injection into the upper crust) versus Cu endowments subdivided by color codes indicating different intervals of magma injection rates. The plot shows that all deposits fall within the interval of magma injection rates ($-3 < \log_{10}[\text{magma injection rate}] < -2.65$) potentially corresponding to large eruptions. The data from porphyry copper deposits (Cu Mt, ore durations and associated 1SD uncertainty bars) are available in Supplementary Data 1. Overall durations of the ore periods are the calculated differences between the oldest and youngest ages of recorded magmatic-hydrothermal mineralizing events with their propagated uncertainties where uncertainties on the above ages are available.

is that there is no fixed threshold of magma injection rate known for large eruptions⁵⁸. Protracted magmatic activity results in the long-term modification of the physical properties of the crust and of the magma within the plumbing system⁵⁸. For instance, the viscosity of the crust decreases with increasing temperature, and the magma within the plumbing system becomes progressively richer in excess fluids. Both these phenomena contribute to dampen the pressure developed by magma injection into the shallow portion of the plumbing system^{58,60,62} thus decreasing the probability of volcanic eruptions⁵⁸. This process could generate conditions that are suitable for the formation of porphyry copper deposits even under high magma injection rates into the upper crust that have been commonly associated with large eruptions.

Our data imply that all supergiant porphyry copper deposits (>10 Mt Cu) are formed by the efficient transfer to upper crustal depths of large magma volumes from the mid- to lower crust³³ with average magma injection rates (i.e., $>0.001 \text{ km}^3 \text{ yr}^{-1}$)^{15,32} that overlap those typically leading to large eruptions^{15,32–34}. Our data support similar conclusions on the formation of the Bingham Canyon deposit, for which magma injection rates of $\geq 0.0065 \text{ km}^3 \text{ yr}^{-1}$, based on thermal and geochemical modelling of zircons⁶⁰, have been proposed (Fig. 5). Since eruption is obviously detrimental to the formation of porphyry copper deposits, our results suggest that supergiant porphyry copper deposits can be considered as failed large eruptions.

Implications for the exploration of supergiant porphyry copper deposits. The above conclusion may have implications on exploration strategies for supergiant (>10 Mt Cu) porphyry copper deposits, both at the field mapping level and concerning the use of rock and mineral fertility tracers. From a field mapping perspective, it has long been recognized that recent caldera structures and associated large ignimbrite deposits are

unfavorable to the formation of porphyry copper deposits³⁶, albeit post-caldera magmatic activity may still lead to relatively small mineralization⁶³. Conversely, volcanic centers (even old calderas) that, in conjunction with geochronology, are demonstrably characterized by protracted magma input during several Myr may be suitable target areas. In fact, they could correspond to the build-up of a large magma reservoir in the upper crust that, under the high magma injection rates discussed above and if accompanied by only small erupted magma volumes, could become the parental reservoir of a supergiant deposit. For instance, the >50 Moz Au high-sulfidation epithermal deposit of Yanacocha and the deeper Kupfertal Cu-Au porphyry are associated with eruption of only $\sim 88 \text{ km}^3$ of volcanic material over a ~ 6 Myr period⁵⁹, which corresponds to a very low average $0.000014 \text{ km}^3 \text{ yr}^{-1}$ eruption rate, almost 2 orders of magnitude less than long-term average magma fluxes in arcs⁶⁴. On the basis of what discussed above, we speculate that old calderas, which inherently witness high magma injection rates, with superimposed long-lived stratovolcanoes characterized by average to low eruption rates could be a potential target for supergiant porphyry copper exploration.

Our results may have implications also on the use of rock and mineral geochemical fertility indicators. In fact, we have shown that both large eruptions and supergiant porphyry copper deposits require the accumulation of similar large magma volumes (from several hundreds to $>1000 \text{ km}^3$) in the upper crust under high magma injection rates (see above and Fig. 1). Recent work suggests that, similarly to porphyry copper deposits, silicic melt segregation from a mid- to lower crustal zone is a pre-requisite for large eruptions⁶⁵ (Fig. 1). All the above points imply broadly similar conditions of magma evolution and storage in the transcrustal magmatic systems leading either to supergiant porphyry copper deposits or to large eruptions, as highlighted in Fig. 1. These magma storage and evolution conditions can be captured by geochemical bulk rock and mineral tracers. Zircon is a particularly powerful tool to decipher physical and chemical magma storage and evolution conditions (e.g., fractionation of pressure-, temperature-, and composition-sensitive minerals, oxygen fugacity) in transcrustal systems and is extensively used as an exploration tool to recognize fertile magmatic systems associated with porphyry copper deposits⁶⁶. Without entering into the details of the meaning of zircon fertility tracers, which is beyond the scope of this study, it is noteworthy that geochemical fertility indices of zircons from subduction-related large eruptions overlap with those of zircons from mineralized porphyry copper deposits (Fig. 7). This supports similar magmatic storage and evolution conditions for porphyry copper deposits and large eruptions (Fig. 1). In contrast, zircons from large eruptions in subduction-unrelated settings display distinct trace element signatures (e.g., Bishop Tuff, rift-related Fig. 7), probably as the result of a range of different magma storage and evolution conditions leading to large eruptions³³. We suggest that improved understanding and further development of petrochronological tracers, able to trace the physico-chemical evolution of transcrustal magmatic systems, may be the key to an improved strategy for the exploration of supergiant porphyry copper deposits.

We argue that the unique association of porphyry copper deposits with the arc environment is the result of a self-constrained process, whereby the arc environment reunites all the geodynamic (subduction-related changes in the overriding plate stress regime^{1,67}), crustal architecture (crust thickness, transcrustal tectonic structures), and geochemical requirements (high H_2O , Cl, S contents of the parental basalts) that favor mineralization. In addition, we also argue that the combination of high magma injection rates, required to form supergiant porphyry copper deposits (this study), thermal pre-conditioning of the crust⁵⁸, and high compressibility of hydrous magmas in the upper crust (all

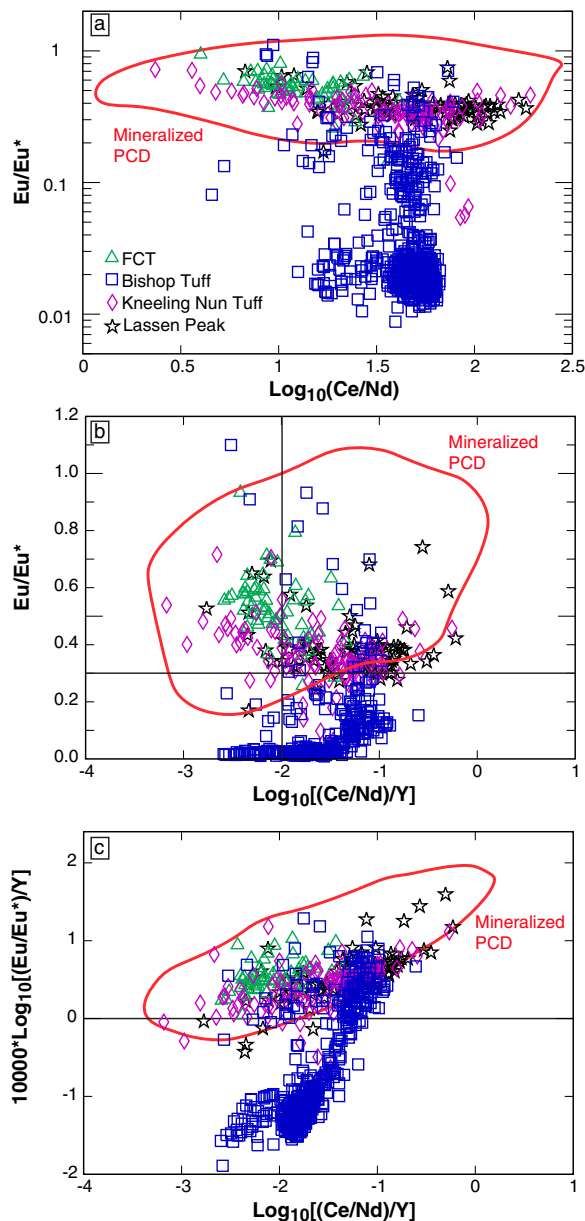


Fig. 7 Trace element plots of zircons from eruptive centers and porphyry copper deposits. Trace element plots of zircons (**a** $\text{Eu}/\text{Eu}^* - \text{Log}_{10}(\text{Ce}/\text{Nd})$; **b** $\text{Eu}/\text{Eu}^* - \text{Log}_{10}[(\text{Ce}/\text{Nd})/\text{Y}]$; **c** $10000 \cdot \text{Log}_{10}[(\text{Eu}/\text{Eu}^*)/\text{Y}] - \text{Log}_{10}(\text{Ce}/\text{Nd})$) from eruptive centers of different geodynamic settings (rift: Bishop Tuff; subduction-related: Lassen Peak, Fish Canyon Tuff, FCT, Kneeling Nun Tuff) compared to the field of zircons associated with porphyry copper deposits and the high-sulfidation epithermal deposit of Yanacocha. The division lines within the plots are from⁶⁶. The porphyry copper deposit field includes zircons from mineralized porphyry intrusions at Butte, Chuquicamata, Escondida, Esperanza, El Salvador, El Teniente, Mirador, Oyu Tolgoi, Yanacocha, and Yerington. Data used in the plot are reported in the Supplementary Data 2.

factors contributing to decrease the likelihood of large eruptions to occur even with high magma injection rates) are optimized in the arc environment. This is due to the hydrous nature of arc magmas and to the peculiar occurrence of long periods of compression in the overriding plate in the syn-subduction setting, different from other settings (e.g., rifting, hot-spot) where the largest eruptions occur³³. Secular changes of the compressive stress field in the thick crust of the overriding plate^{1,67}, associated with large geodynamic processes⁵, could modulate thermal pre-conditioning of the crust,

magma volume transfer and injection rates into the upper crust, that ultimately lead either to the formation of supergiant porphyry copper deposits or to large eruptions.

Methods

Monte Carlo modelling (500000 simulations) was carried out using previous conceptual frameworks^{13,17}.

The starting point of the model is the covariation between potential Cu endowments of magmatic systems (at 50% precipitation efficiency) and magma volumes for the potentially most productive magmatic systems^{13,17}, i.e., those accumulated in the mid- to lower crust (Fig. 1), at pressures of 0.4–1.2 GPa (Fig. 4). Compared to previous works^{13,17}, where the maximum pressure of magma accumulation was 0.9 GPa, we extended the upper pressure limit to 1.2 GPa. Figure 4 shows >10000 simulations and their density distribution. More than 95% of the simulations fall within the two curves of Fig. 4, which are reproduced mathematically by exponential equations of the type

$$\text{MLC_magmaVol} = a * \text{MtCu}^b \quad (1)$$

where parameter “a” ranges randomly between 60 and 700, parameter “b” is defined by the equation

$$b = -0.187767 * \ln(a) + 1.507068 \quad (2)$$

MLC_magmaVol is the mid- to lower crust magma volume corresponding to a specific Cu endowment (within the random range above 0–150 Mt Cu), and “MtCu” is the Cu endowment (at 50% precipitation efficiency) that is allowed to vary randomly between 0 and 150 Mt Cu (Table 1).

Because the longest durations of ore precipitations associated with the largest porphyry copper deposits (i.e., El Teniente 130 Mt Cu, Chuquicamata 106 Mt Cu, Rio Blanco 101 Mt Cu: data from USGS at <https://mrdata.usgs.gov/porcu/>) are <2.0 Myr^{13,17}, we have allowed a maximum time of 2 Myr for the transfer of all magma volumes (including those associated with the maximum potential Cu endowments of 150 Mt Cu) from the mid- to lower crust into the shallow reservoir where fluids exsolve and precipitate Cu with a 50% efficiency (Fig. 1).

Additionally, because geological and geochronological evidences indicate that porphyry copper deposits are formed by repeated magmatic-hydrothermal pulses with durations of few to several tens of kyr, we have allowed magma volume transfer from the mid- to lower crust into the upper crust to occur within any random combination of 5–20 magmatic pulses, each one varying randomly between 2000 and 100000 years. This means that in our model the transfer of any magma volume from the mid- to lower crust into the upper crust can occur from a minimum of 10000 years (5 pulses with a 2000 years duration of each pulse) to a maximum of 2 Myr (20 pulses with a 100000 years duration of each pulse). This random temporal variability for the transfer of any magma volume defined by Eq. (1) above translates into broadly different average magma injection rates that are plotted in Figs. 5, 6.

The volume of each magma pulse is calculated as the ratio between the accumulated magma volume in the mid- to lower crust, that corresponds to a specific Cu endowment and must be transferred to the upper crust to exsolve fluids and Cu, and the random number of pulses (5–20) through which the deep accumulated volume is transferred. Average magma injection rates from the mid- to lower crust into the upper crust are then calculated as the ratios between the volume of the magma pulses and the random durations of each pulse in the interval 2000–100000 years that, incrementally (through the random number of pulses), results in the transfer of the overall magma volume associated with a certain Cu endowment (for 50% precipitation efficiency).

The duration of the injection of magma from the mid- to lower crust into the upper crust (which corresponds to the duration of the ore deposition event, since we assume that each pulse results in an “instantaneous” hydrothermal event) is given by the product of the random number of pulses (5–20) and the random duration of pulses (2000–100000 years).

The full RStudio⁶⁶ script of the Monte Carlo modelling is provided in the Supplementary Note 1.

Data availability

All data generated and discussed during this study are included in this published article and its Supplementary Information (Supplementary Fig. 1, Supplementary Note 1) and Supplementary Data 1 and 2. The data of Supplementary Data 1 on tonnages, magmatic activity and ore durations reported in Figs. 2, 3 and 6 have been deposited on the “Figshare” online open access repository at <https://doi.org/10.6084/m9.figshare.19518133.v4>. The zircon geochemistry data of Supplementary Data 2 have been deposited on the “Figshare” online open access repository at <https://doi.org/10.6084/m9.figshare.19534342.v2>.

Code availability

The script used for Monte Carlo petrologic simulations is reported in Supplementary Note 1 and can be run with RStudio. The RStudio code is also deposited on the “figshare” online open access repository at <https://doi.org/10.6084/m9.figshare.19534204.v1>.

Received: 23 August 2021; Accepted: 14 April 2022;
Published online: 06 May 2022

References

- Tosdal, R. M. & Richards, J. P. Magmatic and Structural Controls on the Development of Porphyry Cu ± Mo ± Au Deposits. <https://doi.org/10.5382/Rev.14.06> (2001).
- Richards, J. P. Postsubduction porphyry Cu-Au and epithermal Au deposits: Products of remelting of subduction-modified lithosphere. *Geology* **37**, 247–250 (2009).
- Richards, J. P. A shake-up in the porphyry world? *Economic Geology* **113**, 1225–1233 (2018).
- Rohrlach, B. D. & Loucks, R. R. Multi-Million-Year Cyclic Ramp-up of Volatiles in a Lower Crustal Magma Reservoir Trapped Below the Tampakan Copper-Gold Deposit by Mio-Pliocene Crustal Compression in the Southern Philippines. In *Super Porphyry Copper & Gold Deposits - A Global Perspective* vol. 2 369–407 (PGC Publishing, 2005).
- Cooke, D. R., Hollings, P. & Walshe, J. L. Giant porphyry deposits: Characteristics, distribution, and tectonic controls. *Econ. Geol.* **100**, 801–818 (2005).
- Rosenbaum, G. et al. Subduction of the Nazca Ridge and the Inca Plateau: Insights into the formation of ore deposits in Peru. *Earth Planetary Sci. Lett.* **239**, 18–32 (2005).
- Zajacz, Z., Seo, J. H., Candela, P. A., Piccoli, P. M. & Tossel, J. A. The solubility of copper in high-temperature magmatic vapors: A quest for the significance of various chloride and sulfide complexes. *Geochimica et Cosmochimica Acta.* **75**, 2811–2827 (2011).
- Richards, J. P. Giant ore deposits formed by optimal alignments and combinations of geological processes. *Nat. Geosci.* **6**, 911–916 (2013).
- Wilkinson, J. J. Triggers for the formation of porphyry ore deposits in magmatic arcs. *Nat. Geosci.* **6**, 917–925 (2013).
- Loucks, R. R. Distinctive composition of copper-ore-forming arc magmas. *Australian J. Earth Sci.* **61**, 5–16 (2014).
- Du, J. & Audétat, A. Early sulfide saturation is not detrimental to porphyry Cu-Au formation. *Geology* **48**, 519–524 (2020).
- Lee, C.-T. A. & Tang, M. How to make porphyry copper deposits. *Earth Planetary Sci. Lett.* **529**, 115868 (2020).
- Chiaradia, M. Gold endowments of porphyry deposits controlled by precipitation efficiency. *Nat. Commun.* **11**, 248 (2020).
- Chiaradia, M. How much water in basaltic melts parental to porphyry copper deposits? *Front. Earth Sci.* **8**, 1–12 (2020).
- Caricchi, L., Simpson, G. & Schaltegger, U. Zircons reveal magma fluxes in the Earth's crust. *Nature* **511**, 457–461 (2014).
- Chelle-Michou, C., Rottier, B., Caricchi, L. & Simpson, G. Tempo of magma degassing and the genesis of porphyry copper deposits. *Scientific Rep.* **7**, 40566 (2017).
- Chiaradia, M. & Caricchi, L. Stochastic modelling of deep magmatic controls on porphyry copper deposit endowment. *Scientific Rep.* **7**, 44523 (2017).
- Park, J.-W., Campbell, I. H., Chiaradia, M., Hao, H. & Lee, C.-T. Crustal magmatic controls on the formation of porphyry copper deposits. *Nat. Rev. Earth. Environ.* **2**, 542–557 (2021).
- Lee, C.-T. A. et al. Copper Systematics in Arc Magmas and Implications for Crust-Mantle Differentiation. *Science* **336**, 64–68 (2012).
- Chiaradia, M. Copper enrichment in arc magmas controlled by overriding plate thickness. *Nat. Geosci.* **7**, 43–46 (2014).
- Audétat, A. The Metal Content of Magmatic-Hydrothermal Fluids and Its Relationship to Mineralization Potential. *Econ. Geol.* **114**, 1033–1056 (2019).
- Cloos, M. Bubbling magma chambers, cupolas, and porphyry copper deposits. *Int. Geol. Rev.* **43**, 285–311 (2001).
- Steinberger, I., Hinks, D., Driesner, T. & Heinrich, C. A. Source Plutons driving porphyry copper ore formation: combining geomagnetic data, thermal constraints, and chemical mass balance to quantify the magma chamber beneath the Bingham canyon deposit. *Econ. Geol.* **108**, 605–624 (2013).
- Core, D. P., Kesler, S. E. & Essene, E. J. Unusually Cu-rich magmas associated with giant porphyry copper deposits: Evidence from Bingham, Utah. *Geology* **34**, 41–44 (2006).
- Stern, C. R., Skewes, M. A. & Arévalo, A. Magmatic evolution of the Giant El Teniente Cu–Mo Deposit, Central Chile. *J. Petrol.* **52**, 1591–1617 (2011).
- Reich, M. et al. Adakite-like signature of Late Miocene intrusions at the Los Pelambres giant porphyry copper deposit in the Andes of central Chile: metallogenic implications. *Miner. Deposita* **38**, 876–885 (2003).
- Rabbia, O. M., Correa, K. J., Hernández, L. B. & Ulrich, T. “Normal” to adakite-like arc magmatism associated with the El Abra porphyry copper deposit, Central Andes, Northern Chile. *Int. J. Earth Sci. (Geol Rundsch)* **106**, 2687–2711 (2017).
- Nathwani, C. L. et al. From long-lived batholith construction to giant porphyry copper deposit formation: petrological and zircon chemical evolution of the Quellaveco District, Southern Peru. *Contrib. Mineral Petrol.* **176**, 12 (2021).
- Newman, S. & Lowenstern, J. B. VolatileCalc: a silicate melt–H₂O–CO₂ solution model written in Visual Basic for excel. *Comp. Geosci.* **28**, 597–604 (2002).
- Sillitoe, R. H. Porphyry copper systems*. *Econ. Geol.* **105**, 3–41 (2010).
- Mercer, C. N., Reed, M. H. & Mercer, C. M. Time Scales of Porphyry Cu Deposit Formation: Insights from Titanium Diffusion in Quartz. *Econ. Geol.* **110**, 587–602 (2015).
- Annen, C. From plutons to magma chambers: Thermal constraints on the accumulation of eruptible silicic magma in the upper crust. *Earth Planetary Sci. Lett.* **284**, 409–416 (2009).
- Wilson, C. J. N. et al. No single model for supersized eruptions and their magma bodies. *Nat. Rev. Earth Environ.* 1–18 <https://doi.org/10.1038/s43017-021-00191-7> (2021).
- Reid, M. R. How long does it take to supersize an eruption? *Elements* **4**, 23–28 (2008).
- Miller, C. F. & Wark, D. A. Supervolcanoes and their explosive supereruptions. *Elements* **4**, 11–15 (2008).
- Sillitoe, R. H. Cauldron subsidence as a possible inhibitor of porphyry copper formation. *Mining Geol. Spec. Issue* **8**, 85–93 (1980).
- Pasteris, J. D. Mount Pinatubo volcano and “negative” porphyry copper deposits. *Geology* **24**, 1075–1078 (1996).
- Korges, M., Weis, P. & Andersen, C. The role of incremental magma chamber growth on ore formation in porphyry copper systems. *Earth Planetary Sci. Lett.* **552**, 116584 (2020).
- Kokh, M. A. et al. Combined effect of carbon dioxide and sulfur on vapor-liquid partitioning of metals in hydrothermal systems. *Geochimica et Cosmochimica Acta.* **187**, 311–333 (2016).
- Ballard, J. R., Palin, J. M., Williams, I. S., Campbell, I. H. & Faunes, A. Two ages of porphyry intrusion resolved for the super-giant Chuquicamata copper deposit of northern Chile by ELA-ICP-MS and SHRIMP. *Geology* **29**, 383–386 (2001).
- Barra, F. et al. Timing and formation of porphyry Cu–Mo mineralization in the Chuquicamata district, northern Chile: new constraints from the Toki cluster. *Miner. Deposita* **48**, 629–651 (2013).
- Maksaev, V. et al. New chronology for El Teniente, Chilean Andes, from U–Pb, 40Ar/39Ar, Re–Os, and fission-track dating: Implications for the evolution of a supergiant porphyry Cu–Mo deposit. *Soc. Econ. Geologists Special Publ.* **11**, 15–54 (2004).
- Cannell, J., Cooke, D. R., Walshe, J. L. & Stein, H. Geology, mineralization, alteration, and structural evolution of the El Teniente Porphyry Cu–Mo deposit. *Econ. Geol.* **100**, 979–1003 (2005).
- Deckart, K., Clark, A. H., Cuadra, P. & Fanning, M. Refinement of the time-space evolution of the giant Mio-Pliocene Rio Blanco-Los Bronces porphyry Cu–Mo cluster, Central Chile: new U–Pb (SHRIMP II) and Re–Os geochronology and 40Ar/39Ar thermochronology data. *Miner. Deposita* **48**, 57–79 (2013).
- Seedorff, E. & Einaudi, M. T. Henderson porphyry molybdenum system, Colorado I. Sequence and abundance of hydrothermal mineral assemblages, flow paths of evolving fluids, and evolutionary styles. *Econ. Geol.* **99**, 3–37 (2004).
- Seedorff, E. & Einaudi, M. T. Henderson porphyry molybdenum system, Colorado II. Decoupling of introduction and deposition of metals during geochemical evolution of hydrothermal fluids. *Econ. Geol.* **99**, 39–71 (2004).
- Quadt, Avon et al. Zircon crystallization and the lifetimes of ore-forming magmatic-hydrothermal systems. *Geology* **39**, 731–734 (2011).
- Li, Y., Selby, D., Condon, D. & Tapster, S. Cyclic Magmatic-hydrothermal evolution in porphyry systems: High-Precision U–Pb and Re–Os Geochronology Constraints on the Tibetan Qulong Porphyry Cu–Mo Deposit. *Econ. Geol.* **112**, 1419–1440 (2017).
- Buret, Y. et al. From a long-lived upper-crustal magma chamber to rapid porphyry copper emplacement: Reading the geochemistry of zircon crystals at Bajo de la Alumbrera (NW Argentina). *Earth Planetary Sci. Lett.* **450**, 120–131 (2016).
- Large, S. J. E., Quadt, A., von Wotzlaw, J.-F., Guillong, M. & Heinrich, C. A. Magma Evolution Leading to Porphyry Au–Cu Mineralization at the Ok Tedi Deposit, Papua New Guinea: Trace Element Geochemistry and High-Precision Geochronology of Igneous Zircon. *Econ. Geol.* **113**, 39–61 (2018).
- Cathles, L., Erendi, A. H. J. & Barrie, C. T. How long can a hydrothermal system be sustained by a single intrusive event? *Econ. Geol.* **92**, 766–771 (1997).
- Weis, P., Driesner, T. & Heinrich, C. A. Porphyry-copper ore shells form at stable pressure-temperature fronts within dynamic fluid plumes. *Science* **338**, 1613–1616 (2012).
- Pollard, P. J., Jongens, R., Stein, H., Mark Fanning, C. & Smillie, R. Rapid formation of Porphyry and Skarn Copper-Gold Mineralization in a

- Postsubduction Environment: Re-Os and U-Pb Geochronology of the Ok Tedi Mine, Papua New Guinea. *Econ. Geol.* **116**, 533–558 (2021).
54. Jollands, M. C., Bloch, E. & Müntener, O. New Ti-in-quartz diffusivities reconcile natural Ti zoning with time scales and temperatures of upper crustal magma reservoirs. *Geology* **48**, 654–657 (2020).
55. Audétat, A., Miyajima, N., Wiesner, D. & Audinot, J.-N. Confirmation of slow Ti diffusion in quartz by diffusion couple experiments and evidence from natural samples. *Geology* <https://doi.org/10.1130/G48785.1> (2021).
56. R Core Team. *R: A language and environment for statistical computing*. R Foundation for Statistical Computing, Vienna, Austria. (2013).
57. Schöpa, A. & Annen, C. The effects of magma flux variations on the formation and lifetime of large silicic magma chambers. *J. Geophys. Res.: Solid Earth* **118**, 926–942 (2013).
58. Karakas, O., Degruyter, W., Bachmann, O. & Dufek, J. Lifetime and size of shallow magma bodies controlled by crustal-scale magmatism. *Nat. Geosci.* **10**, 446–450 (2017).
59. Longo, A. A., Dilles, J. H., Grunder, A. L. & Duncan, R. Evolution of Calc-Alkaline Volcanism and Associated Hydrothermal Gold Deposits at Yanacocha, Peru. *Economic Geology* **105**, 1191–1241 (2010).
60. Large, S. J. E. et al. Copper-mineralised porphyries sample the evolution of a large-volume silicic magma reservoir from rapid assembly to solidification. *Earth Planetary Sci. Lett.* **563**, 116877 (2021).
61. Clark, A. H. Are outsize porphyry copper deposits either anatomically or environmentally distinctive? *Soc. Econ. Geologists Special Publ.* **2**, 213–283 (1993).
62. Caricchi, L., Townsend, M., Rivalta, E. & Namiki, A. The build-up and triggers of volcanic eruptions. *Nat. Rev. Earth Environ.* **2**, 458–476 (2021).
63. John, D. A. Supervolcanoes and metallic ore deposits. *Elements* **4**, 22 (2008).
64. Annen, C., Blundy, J. D. & Sparks, R. S. J. The genesis of intermediate and silicic magmas in deep crustal hot zones. *J. Petrol.* **47**, 505–539 (2006).
65. Sparks, S. et al. Time scales for pluton growth, magma chamber formation and super-eruptions. <https://doi.org/10.21203/rs.3.rs-447477/v1> (2022).
66. Lu, Y. et al. Zircon Compositions as a pathfinder for Porphyry Cu± Mo± Au Deposits. *Soc. Econ. Geologists. Special Publ. Series* **19**, 329–347 (2016).
67. Bertrand, G., Guillou-Frottier, L. & Loiselet, C. Distribution of porphyry copper deposits along the western Tethyan and Andean subduction zones: Insights from a paleotectonic approach. *Ore Geol. Rev.* **60**, 174–190 (2014).
68. Simon, A. C., Pettke, T., Candela, P. A., Piccoli, P. M. & Heinrich, C. A. Copper partitioning in a melt–vapor–brine–magnetite–pyrrhotite assemblage. *Geochimica et Cosmochimica Acta.* **70**, 5583–5600 (2006).
69. Cashman, K. V., Sparks, R. S. J. & Blundy, J. D. Vertically extensive and unstable magmatic systems: A unified view of igneous processes. *Science* **355**, 1–9 (2017).

Acknowledgements

This study was funded by the Swiss National Science Foundation (grant N. 200021_169032 to MC).

Author contributions

M.C. designed the research, performed the Monte Carlo simulations, and drafted the figures. M.C. and L.C. interpreted the data and wrote the manuscript.

Competing interests

The authors declare no competing interests.

Additional information

Supplementary information The online version contains supplementary material available at <https://doi.org/10.1038/s43247-022-00440-7>.

Correspondence and requests for materials should be addressed to Massimo Chiaradia.

Peer review information *Communications Earth & Environment* thanks Rui Wang, John Mavrogenes and Jeffrey Hedenquist for their contribution to the peer review of this work. Primary Handling Editors: Maria Luce Frezzotti, Joe Aslin. Peer reviewer reports are available.

Reprints and permission information is available at <http://www.nature.com/reprints>

Publisher's note Springer Nature remains neutral with regard to jurisdictional claims in published maps and institutional affiliations.



Open Access This article is licensed under a Creative Commons Attribution 4.0 International License, which permits use, sharing, adaptation, distribution and reproduction in any medium or format, as long as you give appropriate credit to the original author(s) and the source, provide a link to the Creative Commons license, and indicate if changes were made. The images or other third party material in this article are included in the article's Creative Commons license, unless indicated otherwise in a credit line to the material. If material is not included in the article's Creative Commons license and your intended use is not permitted by statutory regulation or exceeds the permitted use, you will need to obtain permission directly from the copyright holder. To view a copy of this license, visit <http://creativecommons.org/licenses/by/4.0/>.

© The Author(s) 2022